eXPRESS Polymer Letters Vol.4, No.5 (2010) 264–274
Available online at www.expresspolymlett.com
DOI: 10.3144/expresspolymlett.2010.34

Polyethylene/synthetic boehmite alumina nanocomposites: Structure, thermal and rheological properties

V. M. Khumalo[1], *J. Karger-Kocsis*[1,2*], *R. Thomann*[3]

[1]Department of Polymer Technology, Faculty of Mechanical Engineering and Built Environment, Tshwane University of Technology, Pretoria 0001, Republic of South Africa
[2]Department of Polymer Engineering, Faculty of Mechanical Engineering, Budapest University of Technology and Economics, H-1111 Budapest, Hungary
[3]Institut für Makromolekulare Chemie und Freiburger Materialforschungszentrum, Albert-Ludwigs-Universität Freiburg, Stefan-Meier-Str. 31, D-79104 Freiburg, Germany

Received 9 February 2010; accepted in revised form 4 March 2010

Abstract. Synthetic boehmite alumina (BA) has been incorporated up to 8 wt% in low density polyethylene (LDPE) and high density polyethylene (HDPE), respectively, by melt compounding. The primary nominal particle size of these two BA grades was 40 and 60 nm, respectively. The dispersion of the BA in polyethylene (PE) matrices was investigated by scanning and transmission electron microscopy techniques (SEM and TEM). The thermal (melting and crystallization), thermooxidative (oxidation induction temperature and time), and rheological behaviors of the nanocomposites were determined. It was found that BA is nanoscale dispersed in both LDPE and HDPE without any surface treatment and additional polymeric compatibilizer. BA practically did not influence the thermal (melting and crystallization) and rheological properties of the parent PEs. On the other hand, BA worked as a powerful thermooxidative stabilizer for LDPE, and especially for HDPE nanocomposites.

Keywords: *nanocomposite, polyethylene, boehmite alumina, thermooxidative stability, nanoparticle dispersion*

1. Introduction

Nowadays considerable research efforts are dedicated to produce nanocomposites with improved and/or novel properties compared to the unfilled versions. The nanofillers are either preformed (available initially in nm size range) or produced *in situ* via suitable methods (e.g. sol-gel chemistry, exfoliation of micrometer-sized agglomerates) [1]. Many of the nanofillers are of polar character which can be poorly dispersed in apolar thermoplastics, like polyethylene (PE) and polypropylene (PP). In order to enhance the dispersibility of the nanofillers in polyolefins their surfaces have to be modified by physical (e.g. stearic acid) and chemical treatments (e.g. silane grafting). An alternative and widely practiced way is to use polar polymers as compatibilizers for polyolefin/nanofiller systems. They are usually copolymers in linear and grafted forms. Introduction of compatibilizers is associated, however, with additional costs. Accordingly, researchers are looking for such nanofillers which can be easily and well dispersed without surface treatment and/or additional use of compatibilizers.

Synthetic boehmite alumina (BA) is a very promising candidate in this respect. Its primary particle size is in the range of tens of nanometer. The BA agglomerates can be broken up during melt com-

*Corresponding author, e-mail: karger@pt.bme.hu

pounding as shown recently in case of PP [2, 3]. It is noteworthy that BA is water dispersible and its particles became individually dispersed in the related aqueous media. Siengchin et al. made use of this property of BA and performed water-mediated melt compounding of BA with polyoxymethylene [4], polyamide-6 [5] and PP-based thermoplastic elastomer [6]. The BA, dispersed in water, was introduced in the molten polymer and subsequently evaporated. The latter was facilitated by the screw design of the extruder and by the additional use of a vacuum pump. The dispersion degree of BA was somewhat better for water-mediated than for traditional melt compounding in case of the thermoplastic elastomer [6]. This is a further proof that BA can well be incorporated without any treatment and additional polymeric additive in polyolefins.

BA with the chemical composition of AlO(OH) can be produced in particulates with different aspect ratios. The aspect ratio is increasing according to the ranking: platelet- < rod- < needle-like. The reinforcing and property modification potential of micro- and nanometer-scaled BA, with and without additional surface treatment, has been already checked in various thermoplastics (e.g. [2–13]).

Polyethylenes (PEs) were often modified in the past with nanofillers, like layered silicates in order to improve their mechanical, and especially barrier properties. BA was already incorporated in PE, however, mostly via *in situ* polymerization (i.e. BA served as catalyst support) [14–16]. By this method BA could well be dispersed in PE at very high concentration (up to 40 wt%) .This concentrate was used as PE/BA masterbatch in follow up melt compounding operations [15]. However, compared to studies devoted to PP/BA nanocomposites, less work addressed the effects of BA in polyethylene-based systems.

Accordingly, the present work was aimed at studying the effects of BA in PEs. In order to get a deeper understanding on the structure-property relationships in the related nanocomposites two BA grades and two PE types, viz. low- (LDPE) and high-density PE (HDPE), were involved in this study. The low aspect ratio (platelet-shaped) BA was not surface-modified and its content in the PEs was varied between 0 and 8 wt%.

2. Experimental

2.1. Materials

Disperal® 40 and Disperal® 80 grades of Sasol GmbH (Hamburg, Germany) were used as BA nanofillers. Their characteristics are listed in Table 1.

Table 1. Characteristics of the BAs used

Property	Unit	Disperal® 40	Disperal® 80
Al_2O_3 - content	[%]	82.5	83.4
Surface area	[m^2/g]	105.0	88.0
Loose bulk density	[g/cm^3]	0.57	0.38
Particle size: < 25 μm	[%]	21.0	48.6
Particle size: < 45 μm	[%]	45.4	80.7
Particle size < 90 μm	[%]	92.3	100.0
Crystallite size (021)	[nm]	39.6	74.4
Pore volume total	[ml/g]	0.700	0.870
Median pore size	[nm]	23.3	N/A

LDPE grade LT388 (melt flow index at 190°C/2.16 kg: 10 dg/min; density: 0.922 g/cm^3) from Sasol (Sasolburg, South Africa) and HDPE grade F 7740F2 (melt flow index at 190°C/2.16 kg: 0.4 dg/min; density: 0.946 g/cm^3) from Safripol (Bryanston, South Africa) were used throughout this study.

2.2. Preparation of nanocomposites

Samples of HDPE and LDPE with BA were prepared via melt mixing using a Haake Rheomix OS internal mixer equipped with Polylab OS RheoDrive4 (Thermo Fischer Scientific, Karlsruhe, Germany). Mixing occurred for 8 min at 175°C at 60 rpm for both PEs. Sheets of ca. 2 mm thickness have been produced by compression molding using a Carver press (Wabash, Indiana, USA). The temperature agreed with that of the mixing (=175°C) and the pressure was set for 2 MPa. After ca. 5 min holding time the press was cooled by water and the sheets were demolded.

2.3. Testing

2.3.1. BA dispersion

The dispersion state of the BA particles in the PEs was studied by scanning electron microscopy (SEM) using a FEI Quanta 250 FEG device (FEI, Hillsboro, Oregon, USA). Specimens were cryomicrotomed with a Diatome diamond knife at T = –120°C using a Leica EM UC6 ultramicrotome

equipped with a cryo-chamber. The cryocut surfaces of the specimens were inspected in SEM (acceleration voltage 5 kV) without sputtering, using a high resolution vCD detector for backscattered electrons. The morphology of the samples was also studied in a transmission electron microscope (TEM). The TEM device (Zeiss LEO 912 Omega, Oberkochen, Germany) was working at an acceleration voltage of 120 kV. Thin specimens (ca. 50 nm), prepared by cryocutting with the above ultramicrotome at $T = -120$°C, were subjected to TEM investigations without any staining.

2.3.2. Thermal properties (melting and crystallization)

Differential scanning calorimetric (DSC) tests were run on a PerkinElmer DSC Q2000 (Exton, PA, USA) in the temperature range of 50–200°C. The heating and cooling rates were 20°C/min. The melting peak temperature (T_m), melting enthalpy (ΔH_m), crystallization peak temperature (T_c) and crystallization enthalpy (ΔH_c) were determined. For the 100% crystalline PE a melting enthalpy of ΔH_m = 293 J/g [17] was accepted.

2.3.3. Thermooxidative behavior

Thermogravimetric analysis (TGA) was conducted in a Q500 device of TA Instruments (New Castle, DE, USA) at a heating rate of 20°C/min. Tests were run in oxygen atmosphere in the temperature range from room temperature (*RT*) to 700°C.

The oxygen induction temperature and time (OIT) were determined in a DSC-4 (PerkinElmer DSC 4). Two kinds of tests were made:

– Dynamic OIT (temperature ramp) method: the sample is heated in oxygen at a linear heating rate (10°C/min). The characteristic temperature of the beginning of the oxidation process is determined by the exothermic degradation-induced deviation from the baseline. Note that the scientific literature often prefers the term oxidation onset temperature (OOT) instead of dynamic OIT [18].
– Static OIT (isothermal) method: the sample is heated (from 60°C with 80°C/min) in an inert gas (nitrogen) atmosphere over the melting point to a selected test temperature ($T = 220$°C). This temperature was then kept constant. After reaching the selected temperature (2 min) it has been kept constant for 0.5 min prior to switching the nitrogen gas for oxygen. The oxidative reaction of exothermic feature normally occurs after a certain time period. The OIT value was determined as the time where a deviation from the base line takes place due to the strong exothermic degradation. Because the time was counted from the beginning of the DSC measurement, the OIT value was given by the actual elapsed time – 2.5 min. Recall that 2.5 min was required to reach the isothermal condition of the static OIT measurements.

2.3.4. Rheology

The melt rheology of the nanocomposites was analyzed by an MCR 501 dynamic oscillatory rheometer (Anton Paar Physics, Ostfildern, Germany) working under controlled strain conditions. The test geometry was parallel plate, the diameter of the plates was 25 mm. Compression molded disks of ca. 2 mm thickness were placed between the plates hold at $T = 175$°C. The thickness of the gap was set for 1.5 mm by squeezing the initial PE disk. Frequency sweep tests were carried out at $T = 175$°C. During the measurement a small amplitude (1%) oscillatory shear was applied to the samples. The storage and loss shear moduli ($G'$and G'', respectively) and the dynamic viscosity $|\eta^*|$ were measured as a function of angular frequency (ω) in the range 0.01–100 rad/s.

3. Results and discussion

3.1. BA dispersion

Figure 1 shows SEM pictures taken from the cryocut surfaces of LDPE and HDPE composites with 4 wt% BA40. One can recognize that BA is finely and rather uniformly dispersed in the related matrices.

BA remains in fine dispersion also when introduced in higher amount as demonstrated in Figure 2. The high magnification SEM picture in Figure 2b already indicates that the BA particles are agglomerated. Nevertheless, their mean particle size is on submicrometer scale and thus the related compounds can be termed as nanocomposites.

TEM pictures substantiate that the designation nanocomposite is correctly used (cf. Figure 3). The

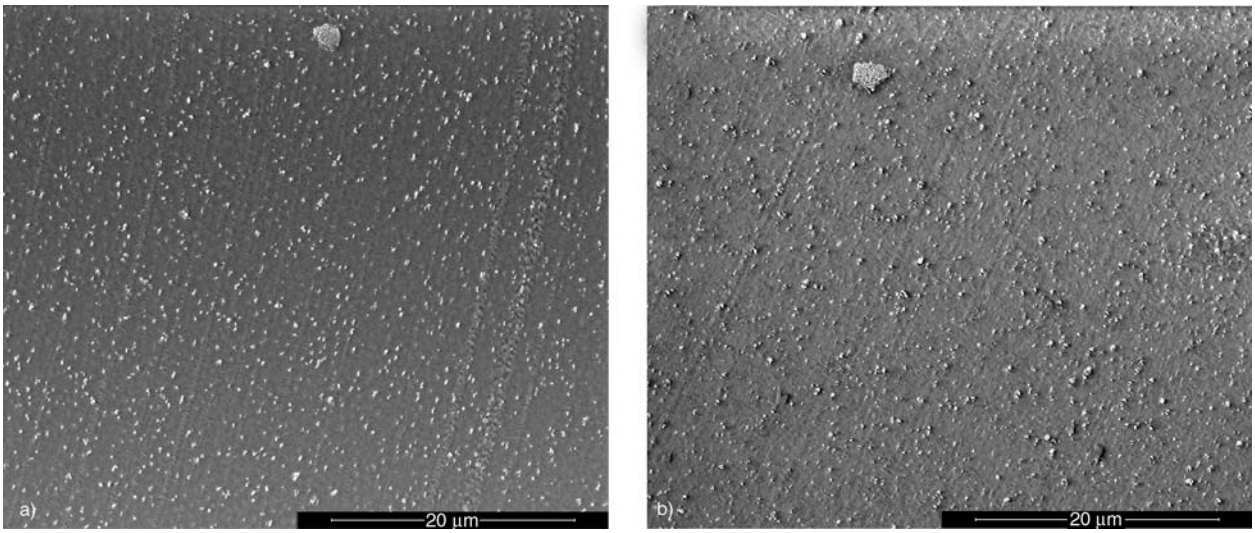

Figure 1. SEM micrographs taken from the cryocut surfaces of LDPE4%BA40 (a) and HDPE4%BA40 (b), respectively

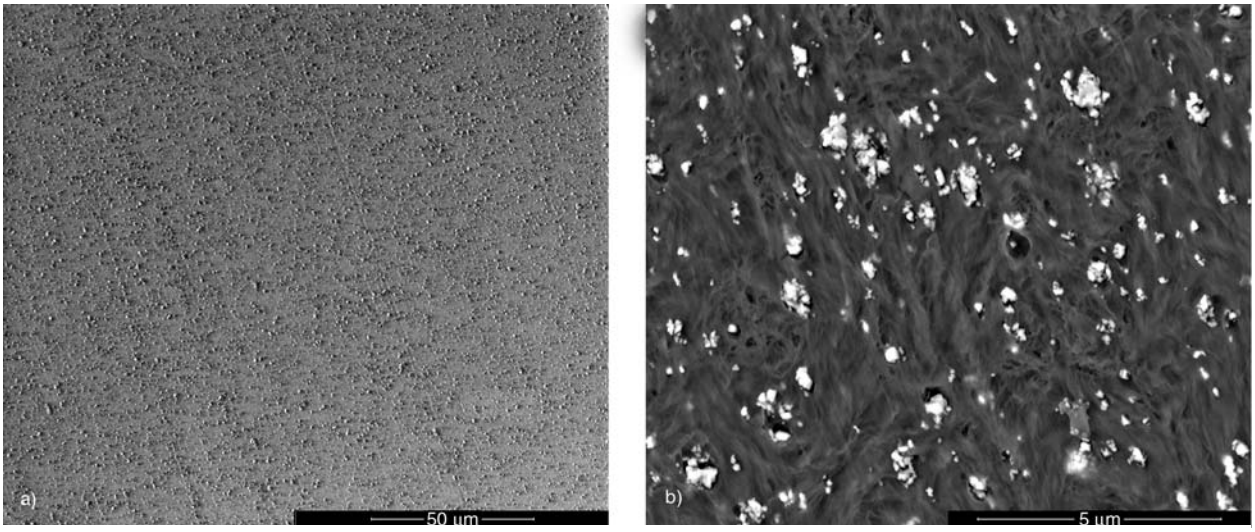

Figure 2. SEM micrographs at various magnifications taken from the cryocut surface of HDPE8%BA80

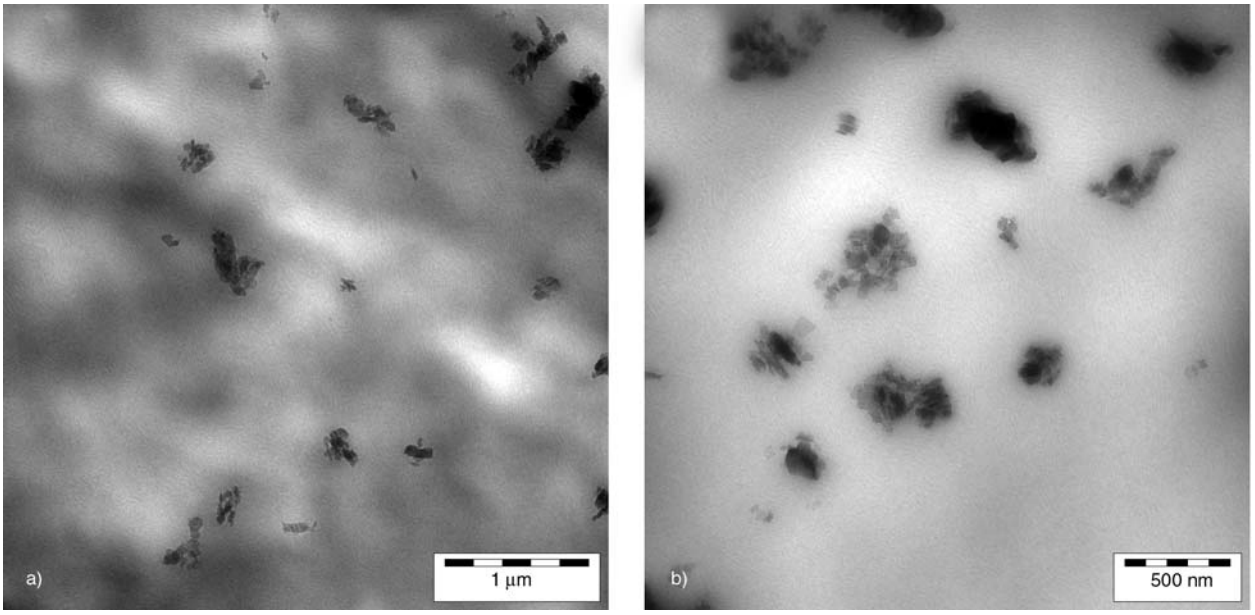

Figure 3. TEM micrographs at various magnifications taken of HDPE4%BA40

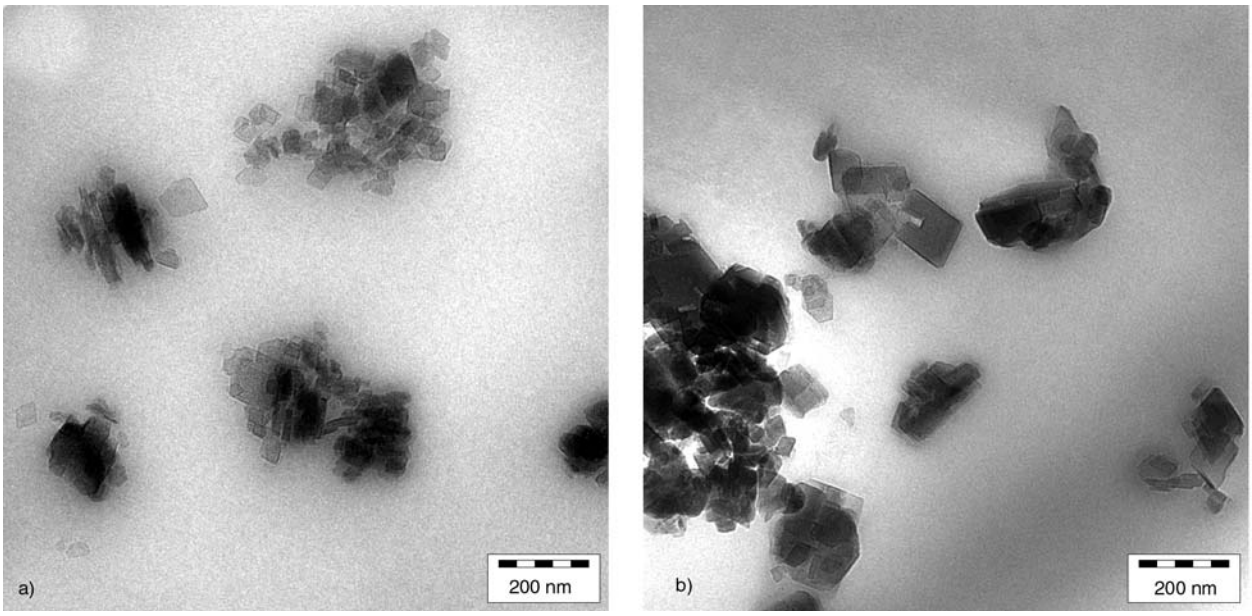

Figure 4. TEM micrographs taken of HDPE4%BA40 (a) and HDPE4%BA80 (b), respectively.
Note: the primary crystallite sizes of BA40 and BA80 are 40 and 74 nm, respectively (cf. Table 1).

difference in the primary crystallite sizes of the BA grades used is well perceptible by comparing the TEM pictures in Figure 4.

The above morphological results confirm that BA can finely be dispersed in PEs even without using coupling agent and polymeric compatibilizer.

3.2. Thermal properties (melting and crystallization)

DSC scans monitored during the 1st and 2nd heating, and cooling are shown for the LDPE/BA40 nanocomposites in Figure 5a and 5b, respectively. It is clearly seen that BA did not affect the melting behavior of the LDPE in the corresponding nanocomposites. A similar conclusion can be drawn by considering the DSC melting traces of the HDPE/BA nanocomposites – cf. Table 2.

However, the crystallization traces in Figure 5b indicate that BA worked as a weak nucleation agent for the crystallization of LDPE. This is obvious due to the shift of the crystallization peak towards higher temperature.

In order to quantify the effects of BA on the melting and crystallization of HDPE and LDPE the DSC traces were analyzed. The melting was characterized by two temperatures, namely peak maximum ($T_{m,\max}$) and final melting ($T_{m,final}$), and the crystallinity value (X_m). The latter was determined by considering the actual melting enthalpy in respect to the 100% crystalline PE (293 J/g as disclosed above [17]). Note that for the crystallinity calculation the BA content of the samples has been considered. The crystallization behavior was characterized again by two temperatures, namely peak maximum ($T_{c,\max}$) and initiation of the crystalliza-

Table 2. Melting and crystallization characteristics of the PE/BA nanocomposites from DSC measurements

Materials	1st melting			Crystallization			2nd melting		
	$T_{m,max}$ [°C]	$T_{m,final}$ [°C]	X_m [%]	$T_{c,max}$ [°C]	$T_{c,initial}$ [°C]	X_m [%]	$T_{m,max}$ [°C]	$T_{m,final}$ [°C]	X_m [%]
Neat HDPE	132.0	145.3	55.3	115.0	119.0	58.0	132.0	147.0	58.0
HDPE4%BA40	131.2	144.3	57.2	116.0	125.0	60.0	132.0	145.5	59.0
HDPE8%BA40	132.0	144.0	58.0	117.3	130.0	56.4	132.2	145.0	58.0
HDPE4%BA80	132.0	145.5	62.0	112.1	119.0	63.1	133.4	149.3	55.1
HDPE8%BA80	131.0	145.0	59.0	116.0	121.4	61.3	132.0	146.3	60.5
Neat LDPE	112.0	127.0	33.2	97.0	104.0	38.4	112.0	126.1	39.0
LDPE4%BA40	111.3	126.1	39.1	98.5	108.0	40.2	111.5	124.0	40.0
LDPE8%BA40	111.0	122.5	37.0	99.1	109.5	37.3	111.0	123.1	37.1
LDPE4%BA80	111.1	124.0	40.3	99.1	110.5	38.2	111.2	126.5	40.0
LDPE8%BA80	111.3	126.0	35.0	99.0	114.0	35.0	111.4	126.1	36.2

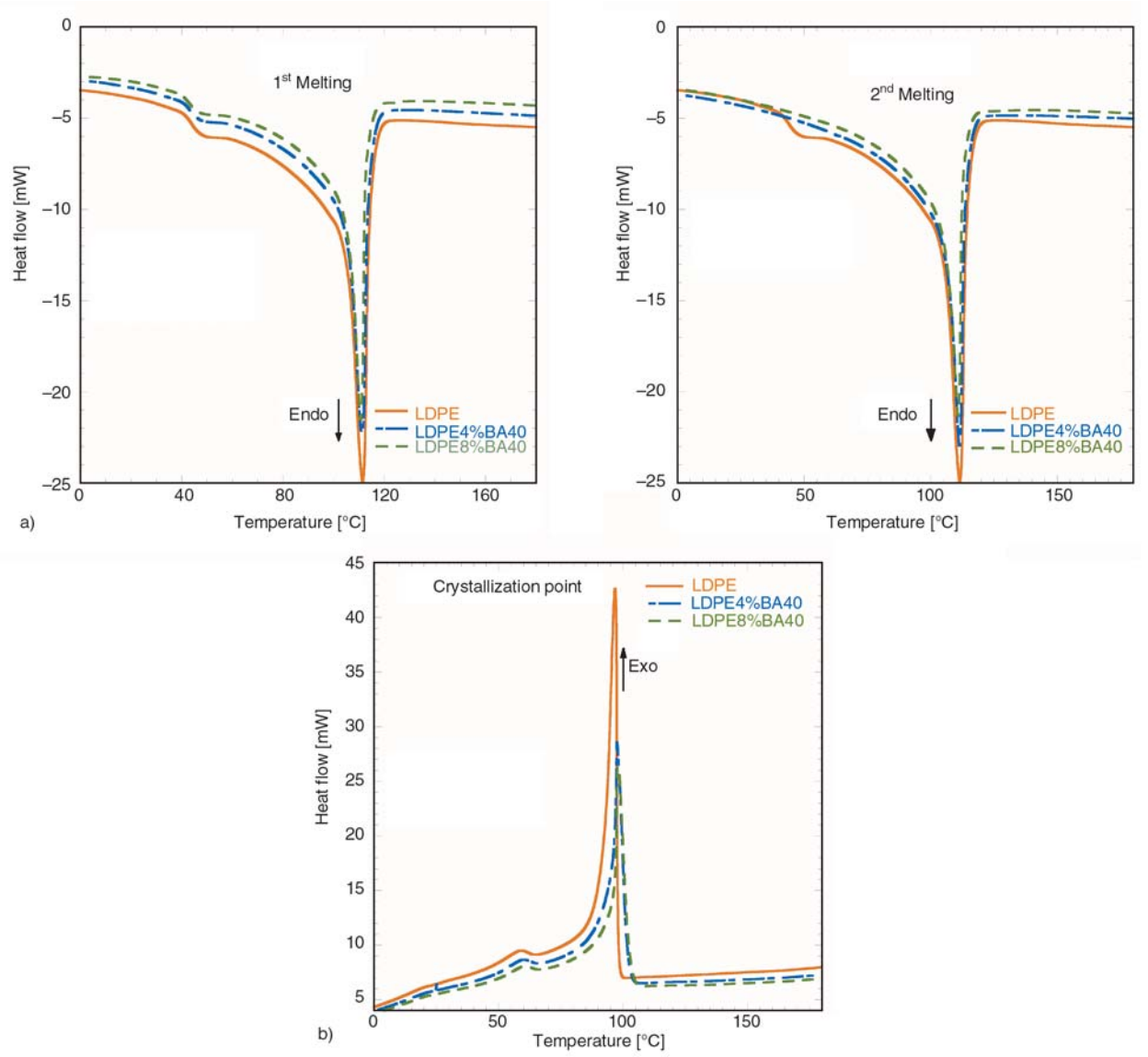

Figure 5. a) DSC heating scans on the LDPE nanocomposites containing 4 and 8 wt% BA40, respectively. Note: heating rate 20°C/min. b) DSC cooling scans on the LDPE nanocomposites containing 4 and 8 wt% BA40, respectively. Note: cooling rate 20°C/min.

tion ($T_{c,initial}$). The crystallinity achieved was also calculated (supposing 293 J/g for the 100% crystallinity). The data related to LDPE and HDPE nanocomposites are summarized in Table 2. It is noteworthy that the weak nucleation effect of BA turns more clearly when $T_{c,initial}$ instead of $T_{c,max}$ values are considered. However, to clarify the nucleation effect of BA on PEs DSC tests at lower cooling rates should be performed.

Data from the 1st heating scans may also suggest that BA increased the crystallinity of both the LDPE and HDPE samples. However results from 2nd heating do not support such effect. It is noteworthy that data from the 2nd heating are relevant as the samples have the same thermal history. BA acted as weak nucleation agent that is proved by the enhanced $T_{c,initial}$ and $T_{c,max}$ values for the PE/BA nanocomposites. It is interesting to note that BA80 was less efficient nucleating agent than BA40 in HDPE. On the other hand, the opposite tendency was observed for the LDPE/BA nanocomposites.

3.3. Thermooxidative properties (TGA, OIT)

3.3.1. TGA

The TGA curves registered for the LDPE and HDPE nanocomposites are displayed in Figures 6 and 7.

One can recognize that the BA acted in most nanocomposites as an additional thermooxidative

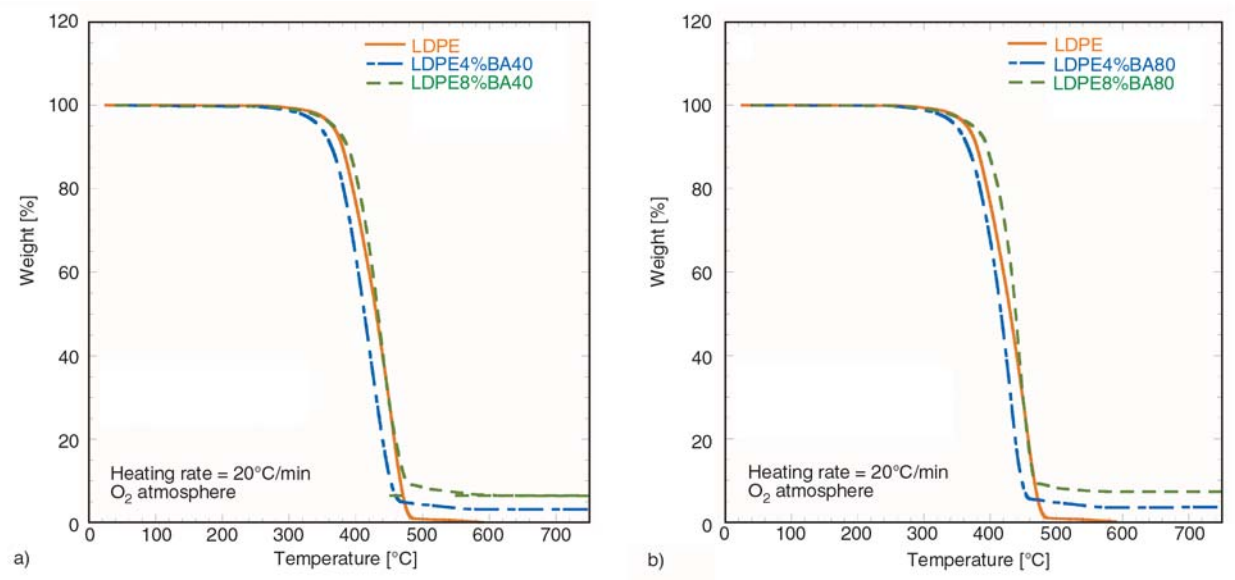

Figure 6. TGA traces of the LDPE nanocomposites with BA40 (a) and BA80 (b)

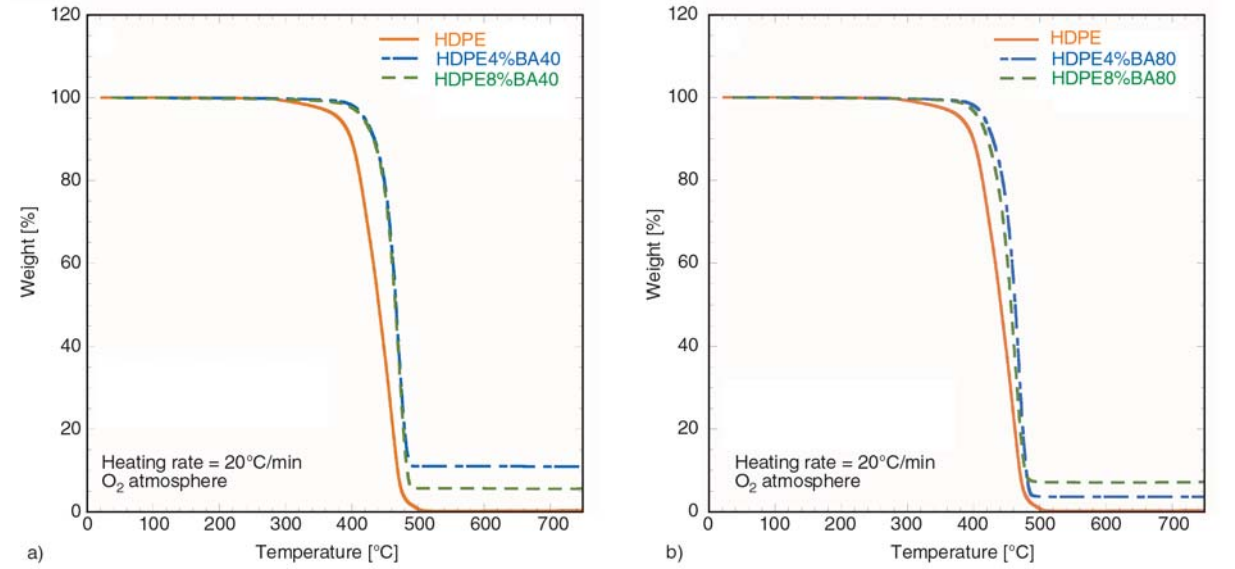

Figure 7. TGA traces of the HDPE nanocomposites with BA40 (a) and BA80 (b)

stabilizer. Its effect was quantified based on the TGA traces by those temperatures which were associated with a weight loss of 2 and 10%, respectively (cf. Table 3). The TGA data in Table 3 dis-

Table 3. TGA and OIT results for the PEs and PE/BA nanocomposites

Materials	TGA			OIT	
	–2 wt% loss [°C]	–10 wt% loss [°C]	Residue [%]	Dynamic [°C]	Static [min]
HDPE Ref	345	400	0.2	235.5	11.0
HDPE4%BA40	347	406	3.4	244.7	21.0
HDPE8%BA40	354	415	6.7	243.8	24.0
HDPE4%BA80	355	408	3.5	–	31.0
HDPE8%BA80	351	423	11.0	–	28.0
LDPE Ref	341	380	0.3	210.8	2.7
LDPE4%BA40	334	381	4.7	–	3.1
LDPE8%BA40	334	387	6.4	215.6	3.0
LDPE4%BA80	338	384	4.6	–	2.6
LDPE8%BA80	352	412	7.1	–	3.2

Notes: – sample not tested. Static OIT data derived from two parallel tests.

play that BA incorporation increased those temperatures where 2 and 10 wt% weight losses, respectively, occurred.

Improved thermooxidative stability owing to the presence of BA has been reported for polyoxymethylene [4]. Interestingly, BA incorporation also improved the stability to photochemical degradation in polyolefins [10, 19]. To clarify the mechanism of BA for improving the thermooxidative stability of PEs (and other polymers) is a very challenging and acute task.

3.3.2. OIT measurements

In order to gain a deeper insight in the thermooxidative action of BA, dynamic and static OIT measurements were performed. The determination of oxidation induction time (OIT_{time}) and oxidation induction temperature (OIT_{temp}) are widely used methods in the thermal analysis of polymers.

Dynamic OIT measurements were aimed at finding a suitable temperature at which the static (i.e. isothermal) OIT tests can be carried out. Figure 8 shows the primary results of the dynamic OIT measurements on the example of LDPE, HDPE, and HDPE8%BA40.

The DSC traces in Figure 8 indicate that the exothermal degradations of HDPE and LDPE start at about 240 and 215°C, respectively. As a consequence we have selected $T = 220$°C to perform the isothermal OIT measurements. It should be noted that $T = 220$°C may be a bit high for LDPE and related nanocomposites and thus differences between their OIT values may not be so pronounced.

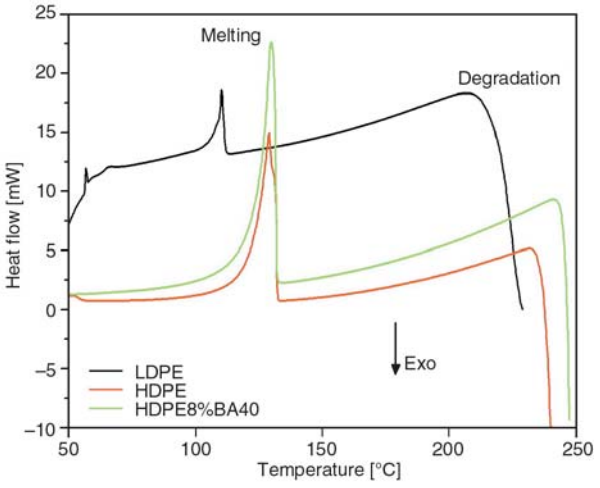

Figure 8. Dynamic OIT measurements on the examples of LDPE, HDPE, and HDPE8%BA40

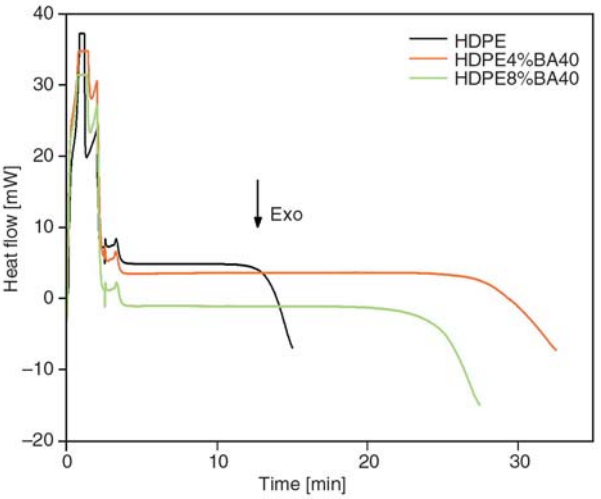

Figure 9. Static (isothermal) OIT curves monitored for HDPE and HDPE/BA40 nanocomposites

Figure 9 displays characteristics static OIT curves registered for HDPE and HDPE/BA nanocomposites.

Figure 9 and the corresponding data in Table 3 already show that the static OIT did not change linearly with the BA content. In addition, according to the TGA results the actual BA content in the sample did not always agree with the nominal BA content. The latter is most probably linked with the sample weight. Nevertheless, BA incorporating enhanced the static OIT. The relative improvement in OIT was more pronounced for HDPE than for LDPE. The improvement in the thermooxidative stability can be explained either by a change in the chemical pathway of the thermal decomposition, or by sorption (physical) effects caused by the nanofiller (e.g. [20]). It is intuitive, that the thermal stability of PE absorbed on the BA surface is higher than that of the bulk due to reduced molecular mobility. This should be valid also for systems with rather weak filler/matrix interaction as in our case. It should also be born in mind, that the volatilization of decomposed gaseous products may also be hampered by the nanofillers of large specific surface area. The feeling of the authors is that the improved thermooxidative stability of PE/BA nanocomposites is due to the abovementioned absorption phenomena. To clarify this effect analytical studies are now in progress. Preliminary results already confirm that the enhanced stability to thermooxidative degradation is related with molecular absorption, in fact.

3.4. Rheological behavior

The rheological tests resulted in unexpected results. Incorporation of nanofillers in thermoplastics (including polyolefins) is generally associated with a marked increase in the melt viscosity, at least in the range of low frequencies (e.g. [21–23]). Parallel to that a steep enhancement in the shear storage modulus (G') can be noticed. These changes are usually assigned to a pseudo solid-like transition caused by the dispersed nanoparticles. The interactions between the nanoparticles and polymer chains hamper the mobility of the latter, increase the friction between them, and thus increase both the viscosity and elasticity of the melt. Moreover, the difference in the melt viscosity and the G' value at low shear rates are often considered as indicators for the fine dispersion and strong particulate filler/matrix interactions (e.g. [23, 24]). However, this is clearly not the case when having a look at the graphs depicted in Figures 10 and 11. The rheological behavior of the systems, as shown in Figures 10 and 11, suggests that there is no strong interaction between the BA and PE in our nanocomposites. This is very beneficial for the processing of such nanocomposites as their melt viscosity practically does not change with either type or amount of BA. To figure out the possible mechanisms behind this finding require, on the other hand, further investigations.

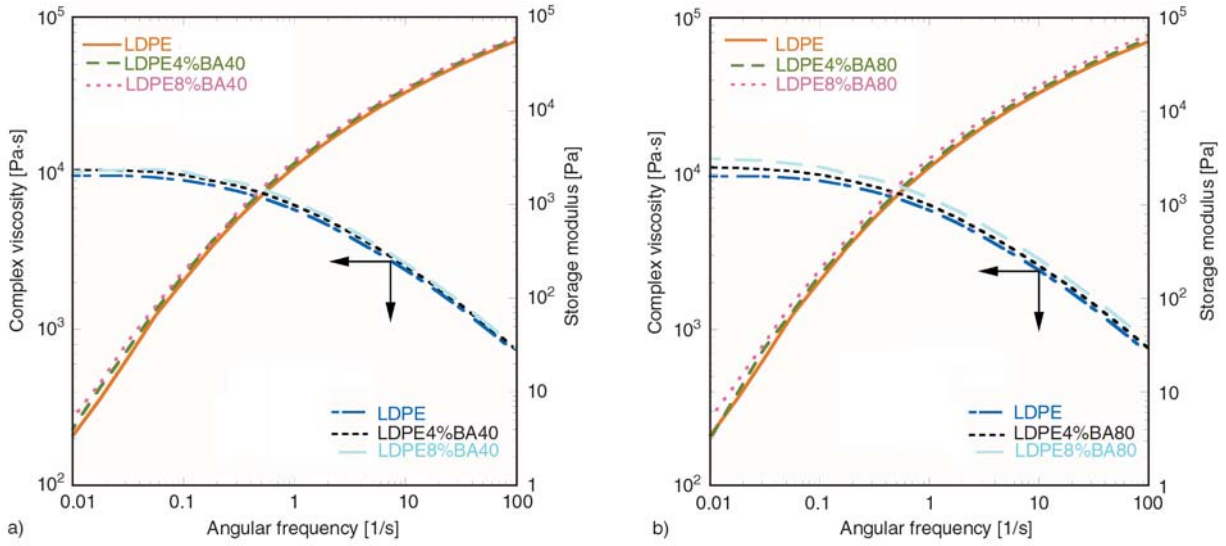

Figure 10. Complex viscosity $|\eta^*|$ and storage modulus (G') vs. angular frequency (ω) for LDPE (a) and LDPE/BA

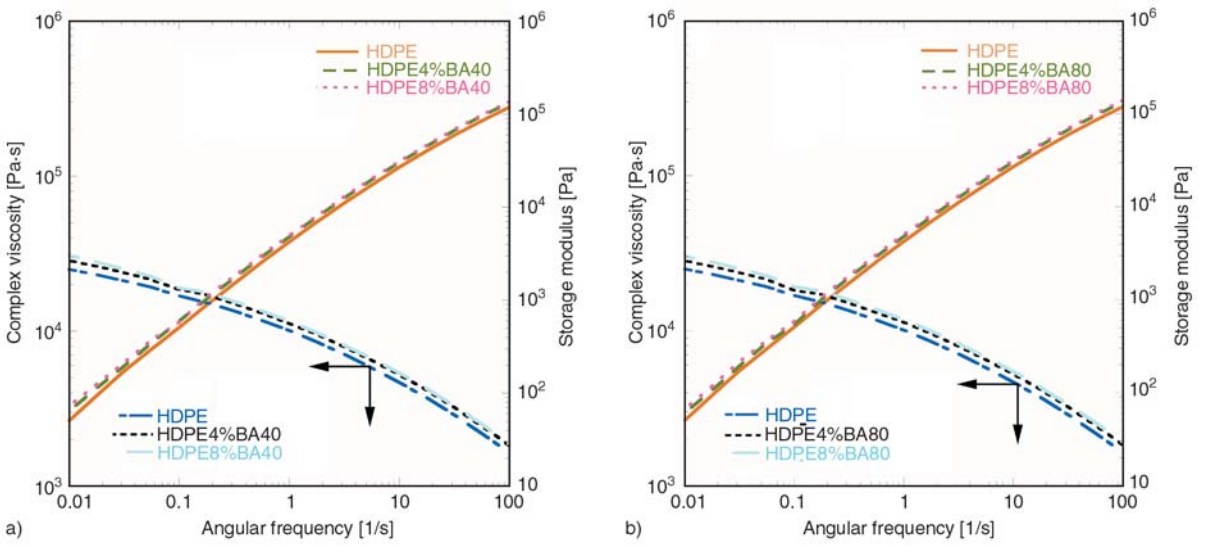

Figure 11. Complex viscosity $|\eta^*|$ and storage modulus (G') vs. angular frequency (ω) for HDPE (a) and HDPE/BA nanocomposites (b)

4. Conclusions

This work was devoted to determine the effects of synthetic boehmite alumina (BA) on the morphology, thermal, thermooxidative and rheological behavior of polyethylenes (PEs). BA was incorporated, up to 8 wt%, in both low- (LDPE) and high-density PE (HDPE) through melt compounding. It was established that BA was finely, and rather uniformly dispersed, though agglomerated, in the corresponding PEs. BA acted as a weak nucleating agent because it reduced slightly the undercooling (difference between the melting and crystallization temperatures) of both LDPE and HDPE. The nucleation capability of BA depended on the type, and in lesser extent also on the amount of the BA incorporated. Filling with BA strongly improved the stability to thermooxidative degradation of the corresponding PE matrix. The stabilizing effect of BA was more pronounced for HDPE than for LDPE. This finding is likely linked with the absorption of PE chains on the BA surface rather than with a synergistic effect of BA with the thermostabilizer initially present in the corresponding PE. Surprisingly, the melt rheology of the PE/BA nanocomposites was well matched with that of the parent PEs. This behavior is seldom for thermoplastic nanocomposites and has great practical relevance (i.e. similar processability as the plain PEs). Further investigations are needed, however, to reason this unexpected rheological performance.

Acknowledgements

The authors are indebted to Profs. S. Sinha Ray and O. C. Vorster (Nanocenter – Council for Scientific and Industrial Research , and Tshwane University of Technology, respectively, both in Pretoria, South Africa) for testing facilities and discussion of the results. The BA delivery, arranged by Dr. O. Torno (Sasol GmbH, Hamburg, Germany), is gratefully acknowledged.

References

[1] Karger-Kocsis J.: On the toughness of 'nanomodified' polymers and their traditional polymer composites. in 'Nano- and micro-mechanics of polymer blends and composites' (eds: Karger-Kocsis J., Fakirov S.) Hanser, Munich, 425–470 (2009).

[2] Streller R. C., Thomann R., Torno O., Mülhaupt R.: Isotactic poly(propylene) nanocomposites based upon boehmite nanofillers. Macromolecular Materials and Engineering, **293**, 218–227 (2008).
DOI: 10.1002/mame.200700354

[3] Streller R. C., Thomann R., Torno O., Mülhaupt R.: Morphology, crystallization behavior, and mechanical properties of isotactic poly(propylene) nanocomposites based on organophilic boehmites. Macromolecular Materials and Engineering, **294**, 380–388 (2009).
DOI: 10.1002/mame.200800360

[4] Siengchin S., Karger-Kocsis J., Thomann R.: Nanofilled and/or toughened POM composites produced by water-mediated melt compounding: Structure and mechanical properties. Express Polymer Letters, **2**, 746–756 (2008).
DOI: 10.3144/expresspolymlett.2008.88

[5] Siengchin S., Karger-Kocsis J.: Structure and creep response of toughened and nanoreinforced polyamides produced via the latex route: Effect of nanofiller type. Composites Science and Technology, **69**, 677–683 (2009).
DOI: 10.1016/j.compscitech.2009.01.003

[6] Siengchin S., Karger-Kocsis J.: Mechanical and stress relaxation behavior of Santoprene® thermoplastic elastomer/boehmite alumina nanocomposites produced by water-mediated and direct melt compounding. Composites Part A: Applied Science and Manufacturing, in press (2010).
DOI: 10.1016/j.compositesa.2010.02.009

[7] Siengchin S., Karger-Kocsis J., Thomann R.: Alumina-filled polystyrene micro- and nanocomposites prepared by melt mixing with and without latex precompounding: Structure and properties. Journal of Applied Polymer Science, **105**, 2963–2972 (2007).
DOI: 10.1002/app.26505

[8] Brostow W., Datashvili T., Huang B., Too J.: Tensile properties of LDPE+boehmite composites. Polymer Composites, **30**, 760–767 (2009).
DOI: 10.1002/pc.20610

[9] Brostow W., Datashvili T., Kao D., Too J.: Tribological properties of LDPE+boehmite composites. Polymer Composites, **31**, 417–425 (2010).
DOI: 10.1002/pc.20820

[10] Bocchini S., Morlat-Thérias S., Gardette J-L., Camino G.: Influence of nanodispersed boehmite on polypropylene photooxidation. Polymer Degradation and Stability, **92**, 1847–1856 (2007).
DOI: 10.1016/j.polymdegradstab.2007.07.002

[11] Özdilek C., Kazimierczak K., van der Beek D., Picken S. J.: Preparation and properties of polyamide-6-boehmite nanocomposites. Polymer, **45**, 5207–5214 (2004).
DOI: 10.1016/j.polymer.2004.05.029

[12] Özdilek C., Mendes E., Picken S. J.: Nematic phase formation of boehmite in polyamide-6 nanocomposites. Polymer, **47**, 2189–2197 (2006).
DOI: 10.1016/j.polymer.2006.01.043

[13] Özdilek C., Norder B., Picken S. J.: A study of the thermo-mechanical behavior of boehmite-polyamide-6 nanocomposites. Thermochimica Acta, **472**, 31–37 (2008).
DOI: 10.1016/j.tca.2008.03.008

[14] Xalter R., Pelascini F., Mülhaupt R.: Ethylene polymerization, on-line particle growth monitoring, and *in situ* nanocomposite formation using catalysts supported on arylsulfonic acid-modified boehmites. Macromolecules, **41**, 3136–3143 (2008).
DOI: 10.1021/ma702623e

[15] Halbach T. S., Thomann Y., Mülhaupt R.: Boehmite nanorod-reinforced-polyethylenes and ethylene/1-octene thermoplastic elastomer nanocomposites prepared by *in situ* olefin polymerization and melt compounding. Journal of Polymer Science Part A: Polymer Chemistry, **46**, 2755–2765 (2008).
DOI: 10.1002/pola.22608

[16] Halbach T. S., Mülhaupt R.: Boehmite-based polyethylene nanocomposites prepared by in-situ polymerization. Polymer, **49**, 867–876 (2008).
DOI: 10.1016/j.polymer.2007.12.007

[17] Wunderlich B., Dole M.: Specific heat of synthetic high polymers. VIII Low pressure polyethylene. Journal of Polymer Science, **24**, 201–212 (1957).
DOI: 10.1002/pol.1957.1202410604

[18] Focke W. W., van der Westhuizen I.: Oxidation induction time and oxidation onset temperature of polyethylene in air. Journal of Thermal Analysis and Calorimetry, **99**, 285–293 (2010).
DOI: 10.1007/s10973-009-0097-1

[19] Chmela S., Fiedlerová A., Borsig E., Erler J., Mülhaupt R.: Photo-oxidation and stabilization of sPP and iPP/boehmite-disperal nanocomposites. Journal of Macromolecular Science Part A: Pure and Applied Chemistry, **44**, 1027–1034 (2007).
DOI: 10.1080/10601320701424461

[20] Zou D. Q., Yoshida H.: Size effect of silica nanoparticles on thermal decomposition of PMMA. Journal of Thermal Analysis and Calorimetry, **99**, 21–26 (2010).
DOI: 10.1007/s10973-009-0531-4

[21] Durmus A., Kasgoz A., Macosko C. W.: Linear low density polyethylene (LLDPE)/clay nanocomposites. Part I: Structural characterization and quantifying clay dispersion by melt rheology. Polymer, **48**, 4492–4502 (2007).
DOI: 10.1016/j.polymer.2007.05.074

[22] Rezanavaz R., Razavi Aghjeh M. K., Babaluo A. A.: Rheology, morphology, and thermal behavior of HDPE/clay nanocomposites. Polymer Composites, in press (2010).
DOI: 10.1002/pc.20889

[23] Dorigato A., Pegoretti A., Penati A.: Linear low-density polyethylene/silica micro- and nanocomposites: Dynamic rheological measurements and modeling. Express Polymer Letters, **4**, 115–129 (2010).
DOI: 10.3144/expresspolymlett.2010.16

[24] Chow W. S., Mohd Ishak Z. A., Karger-Kocsis J.: Morphological and rheological properties of polyamide 6/poly(propylene)/organoclay nanocomposites. Macromolecular Materials and Engineering, **290**, 122–127 (2005).
DOI: 10.1002/mame.200400269